Characterisation of Irradiation-Induced Defects in ZnO Single Crystals

Ivan Procházka[1], Jakub Čížek[1], František Lukáč[1], Oksana Melikhova[1], Jan Valenta[1], Vladimír Havránek[2], Wolfgang Anwand[3], Vladimir A. Skuratov[4], Tatiana S. Strukova[4]

[1] *Faculty of Mathematics and Physics, Charles University in Prague, Prague, Czech Republic*

[2] *Nuclear Physics Institute, Academy of Science of the Czech Republic, Řež, Czech Republic*

[3] *Institute of Radiation Physics, Helmholtz-Zentrum Dresden-Rossedorf, Dresden, Germany*

[4] *Flerov Laboratory of Nuclear Reactions, JINR Dubna, Russian Federation*

PSD-14, September 14 – 19, 2014, Kyoto, Japan

Talk structure

- Introduction & motivation.
- Experimental part.
- Results & discussion.
- Summary.
- Acknowledgements.

Introduction & motivation

Zinc oxide (ZnO):

- a direct wide band gap semiconductor ($E_g \approx 3.37$ eV at ambient conditions),
- a large exciton binding energy ($E_{ex} \approx 60$ meV),
- high-quality ZnO bulk single crystals (pressurized melt gown – MG, hydrothermally grown – HTG crystals),
- a simple and relatively cheap ZnO crystal-growth technology.

⇒ **ZnO is interesting for applications:**

- optoelectronic devices,
- UV light emitting diodes and lasers,
- gas sensors,
- transparent electrodes for solar cells,
- … .

Introduction & motivation

Zinc oxide (ZnO):

- point defects may control functional properties of ZnO,
- grown-in defects and native impurities (especially the hydrogen in HTG ZnO),
- irradiation-induced structure modifications of ZnO materials become of interest: tailoring of desired properties, degradation of functional properties during operation.
- hydrogen can be easily incorporated into ZnO lattice (shallow donor state).

It is important to characterise irradiation-induced structure modifications of zinc oxide.

Introduction & motivation

The aim of the present Contribution:

- implantation of energetic (≈ 100 MeV) Xe ions into bulk HTG ZnO single crystals,
- characterisation of defects introduced in ZnO by Xe implantation,
- comparison of results with those observed after irradiations of ZnO by energetic electrons and protons.

Three experimental techniques were combined:

- positron annihilation spectroscopy,
- optical transmittance,
- photoluminescence.

Experiments

Samples

Virgin ZnO single crystals (MaTecK GmbH):

- HTG ZnO (0001), O-terminated,
- $10\times10\times0.5$ mm^3,
- optically polished surfaces.

Xe ion irradiation (IC-100 cyclotron @ FLNR, JINR Dubna):

- Xe^{26+} , 167 MeV kinetic energy,
- fluencies up to 10^{14} cm^{-2},
- irrad. temperature 50 °C.

Proton irradiation (Tandetron facility @ NPI Rez):

- proton kinetic energy 2.5 MeV,
- fluency 10^{16} cm^{-2},
- irrad. temperature < 100 °C.

Experiments

Samples

SRIM simulations:

depth profiles of ion and defect concentrations.

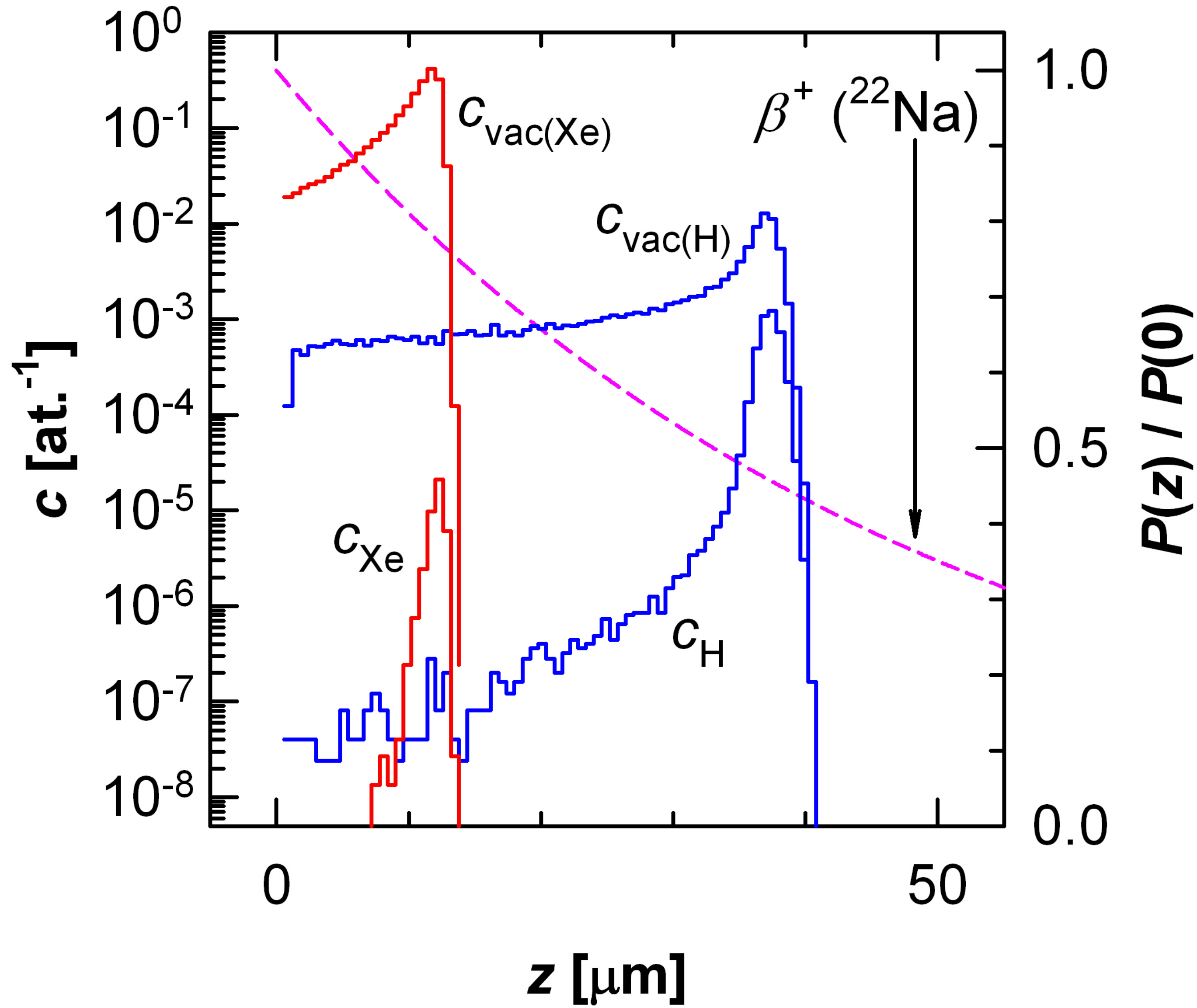

Approx. 57% of ^{22}Na β^+ particles is stopped below 40 µm depth and 20% below 13 µm depth.

Experiments

Positron lifetime spectrometry (LT)

LT spectrometer – Becvar et al., NIMA (2005):

- ^{22}Na positron source (1 MBq) sealed between Mylar ® foils,
- BaF_2 fast scintillator detectors,
- digital processing of the timing signals,
- time resolution of 0.145 ns (fwhm for ^{22}Na), ≈120 coincidence events per second.

sample-source sandwich

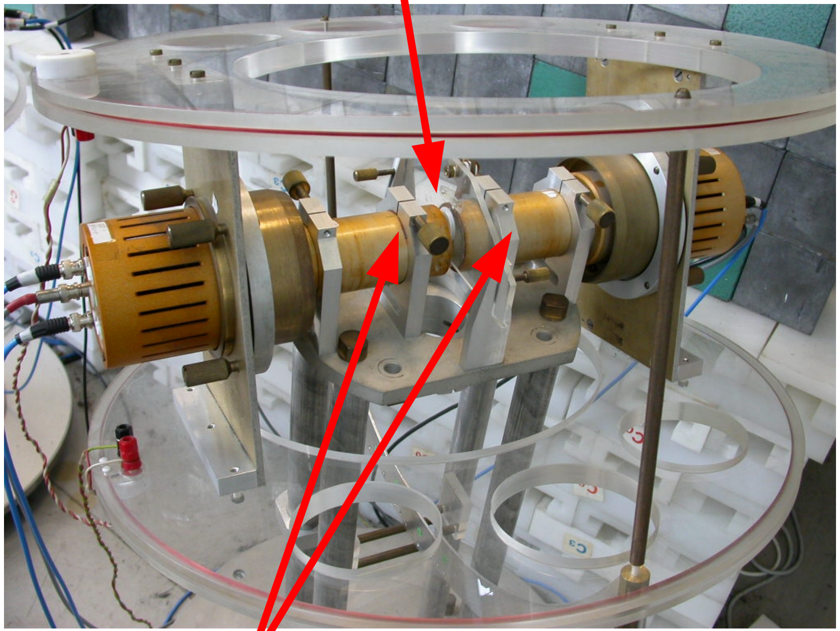

BaF_2 scintillator detectors

At least 10^7 coincidence events collected in each spectrum.

Well-annealed *α*-Fe reference measured for subtracting the contribution from annihilation in the source – sample assembly.

Experiments

Coincidence Doppler broadening measurements (CDB)

CDB spectrometer – Cizek et al., NIMA (2011):

- HPGe–HPGe with digital signal processing,
- energy resolution 0.9 keV at γ-511 keV (FWHM),
- count rate ≈ 550 cc s^{-1}.

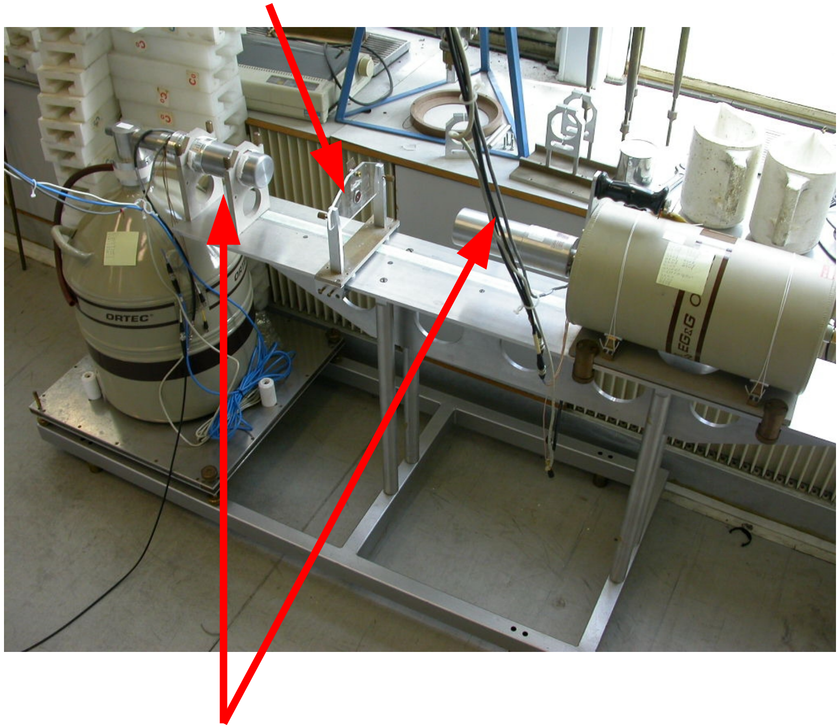

At least 10^8 coincidence events collected in each two-dimensional (2D) spectrum.

DB profiles (DBP) obtained as proper cuts in the 2D spectra.

Experiments

Slow-positron implantation spectroscopy (SPIS)

SPIS apparatus – Brauer et al. (1995), Anwand et al. (2013)

- Magnetically guided positron beam „SPONSOR“ @ HZDR ,
- single-HPGe DB measurements,
- energy resolution 1.03 keV (FWHM) @ *γ*-511 keV.

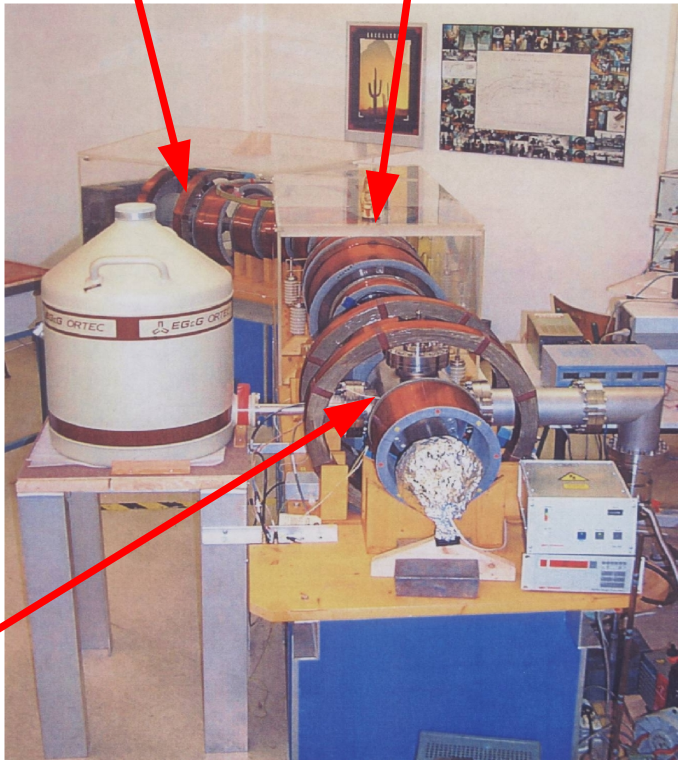

At least 5×10^5 counts collected in each annihilation peak.

Ordinary sharpness (*S*) and wing (*W*) parameters evaluated.

Experiments

Optical transmission (OT)

Spekol instrument (a white light source with a grating monochromator; wavelength *λ* ranged from 340 to 880 nm.

The reflectivity of each crystal was assumed to be independent of *λ*.

Photoluminescence (PL)

- An Olympus IX-71 inverted microscope with an Ealing 25×/0.4 mirror objective lens.
- An ARC SP2300i imagging spectrometer.
- An UV LED lamp light source (325 or 310 nm).
- A LN2-cooled back-illuminated CCD detector.
- The lateral resolution of ≈ 0.5 μm.

Results & discussion

LT measurements – positron lifetimes τ_i and relative intensities I_i							
Sample	**f [cm^{-2}]**	**τ_2 [ps]**	**I_2 [%]**	**τ_3 [ps]**	**I_3 [%]**	**τ_4 [ps]**	**I_4 [%]**
virgin		183.2(1)	100				
Xe^{26+} irrad.	3×10^{12}	184(1)	83.6(8)			369.6(6)	13.7(7)
	3×10^{13}	185.4(5)	78.9(4)			365(2)	21.1(5)
	1×10^{14}	184.1(7)	74.5(8)			351(1)	25.5(7)
	opposite	183(2)	100				
H^+ irrad.	1×10^{16}	175(5)	71(2)	260(2)	29(2)		
	opposite	180(1)	100				

- Saturated positron trapping ($\tau_i > \tau_{bulk} \approx 154$ ps).
- Virgin crystal and unirradiated side of implanted samples – single component only (τ_2).
- Xe^{26+}-irradiated side – τ_2- and τ_4-components.
- H^+-irradiated side – two components (τ_2 and τ_3).

Results & discussion

LT measurements – positron lifetimes τ_i and relative intensities I_i							
Sample	**f [cm^{-2}]**	**τ_2 [ps]**	**I_2 [%]**	**τ_3 [ps]**	**I_3 [%]**	**τ_4 [ps]**	**I_4 [%]**
virgin		183.2(1)	100				
Xe^{26+} irrad.	3×10^{12}	184(1)	83.6(8)			369.6(6)	13.7(7)
	3×10^{13}	185.4(5)	78.9(4)			365(2)	21.1(5)
	1×10^{14}	184.1(7)	74.5(8)			351(1)	25.5(7)
	opposite	183(2)	100				
H^+ irrad.	1×10^{16}	175(5)	71(2)	260(2)	29(2)		
	opposite	180(1)	100				

- Origin of the τ_2- and τ_3-components, Brauer et al., PR B (2009):

  τ_2 – zinc vacancy decorated with H atom (V_{Zn} – 1H),
  τ_3 – zinc and oxygen vacancy complex (V_{Zn} – V_O divacancy).
- Origin of the τ_4-component – larger clusters of V_{Zn} and/or V_O (approx. 10 vacancies).

Results & discussion

ATSUP calculations:

- Boroński-Nieminen (BN) approximation to e^+ - e^- correlation,
- atomic relaxations,
- shortened $\tau(V_{Zn})$ due to hydrogen attachment.

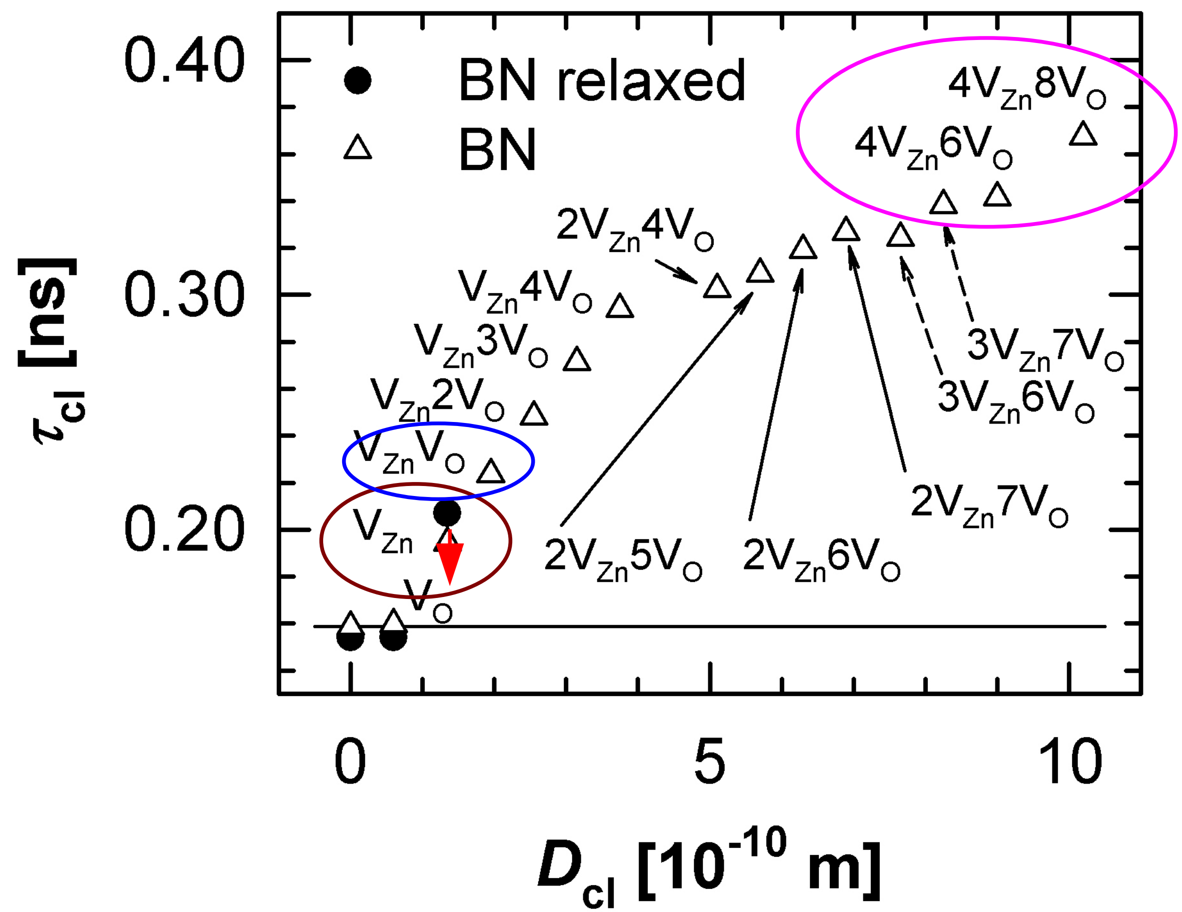

- Origin of the τ_2- and τ_3-components, Brauer et al., PR B (2009):

  τ_2 – zinc vacancy decorated with H atom (V_{Zn} – 1H),
  τ_3 – zinc and oxygen vacancy complex (V_{Zn} – V_O divacancy).

- Origin of the τ_4-component – larger clusters of V_{Zn} and/or V_O (approx. 10 vacancies).

Results & discussion

CDB results

In both virgin and Xe-irradiated samples, the contribution of oxygen 2p electrons dominates at the positron annihilation sites.

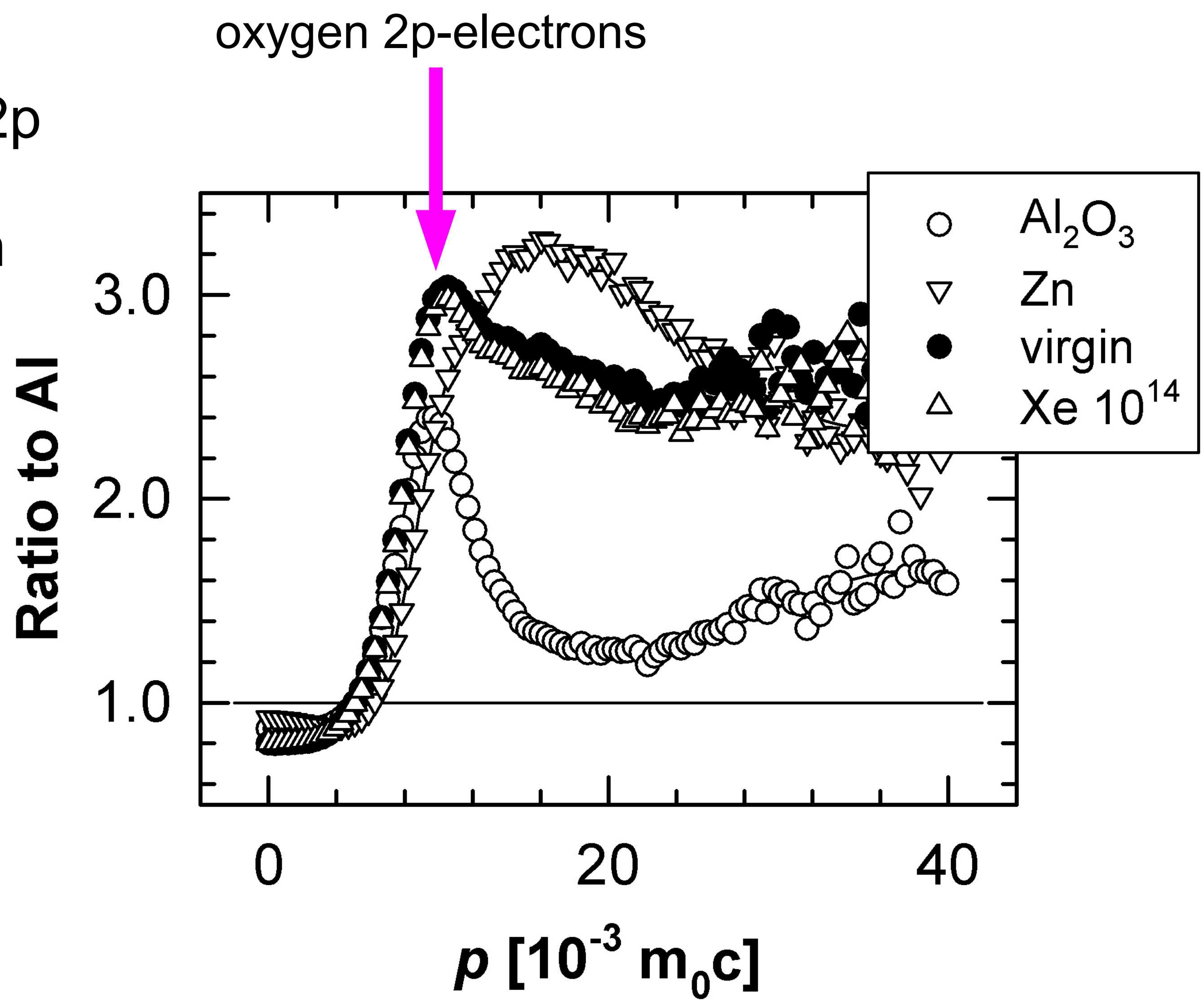

Results & discussion

SPIS results:

VEPFIT analysis (model #5, single layer):

virgin – L_+=58(2) nm,

H^+ implanted (1×10^{16} cm^{-2}) – L_+=19(2) nm,

Xe^{26+} implanted (1×10^{14} cm^{-2}) – L_+=47(2) nm.

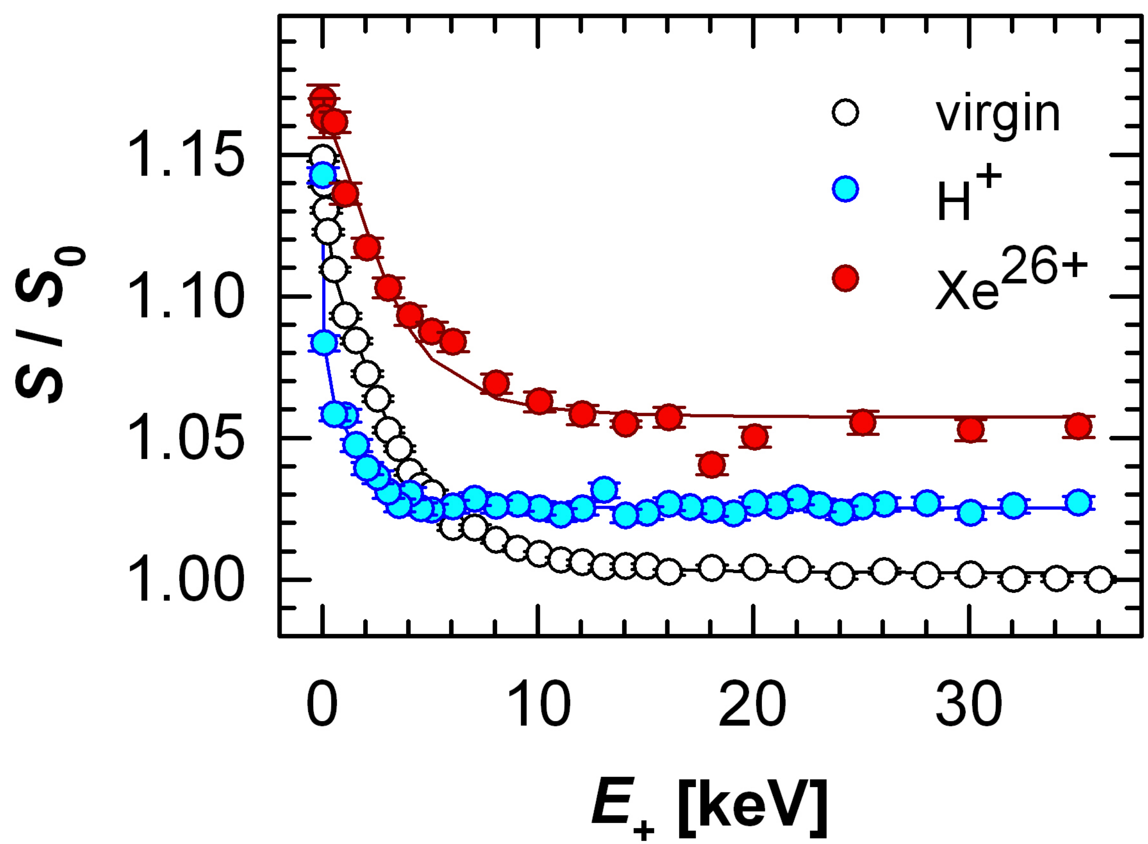

Results & discussion

Combination of LT and SPIS results

Estimates of concentrations of clusters induced by Xe^{26+} irradiation:

$$c_{V_{Zn}-H} = \frac{1}{\mu_V \tau_B}\left(\frac{L_{+,B}^2}{L_+^2} - 1\right)$$

$$c_{cl} = \frac{1}{f}\,\frac{I_4}{I_2}\,\frac{\Omega_V}{\Omega_{cl}}\,\mu_V\, c_{V_{Zn}-H}$$

$$\mu_V \approx 1\times10^{15}\ \ \mathrm{s}^{-1}$$
$$\tau_B = 154\ \ \mathrm{ps}$$
$$\Omega_{4V_{Zn}-8V_O}/\Omega_V \approx 4.7$$
$$f \approx 0.21$$

$$c_{V_{Zn}-H} \approx 7\times10^{-5}\ \ \mathrm{at.}^{-1}$$

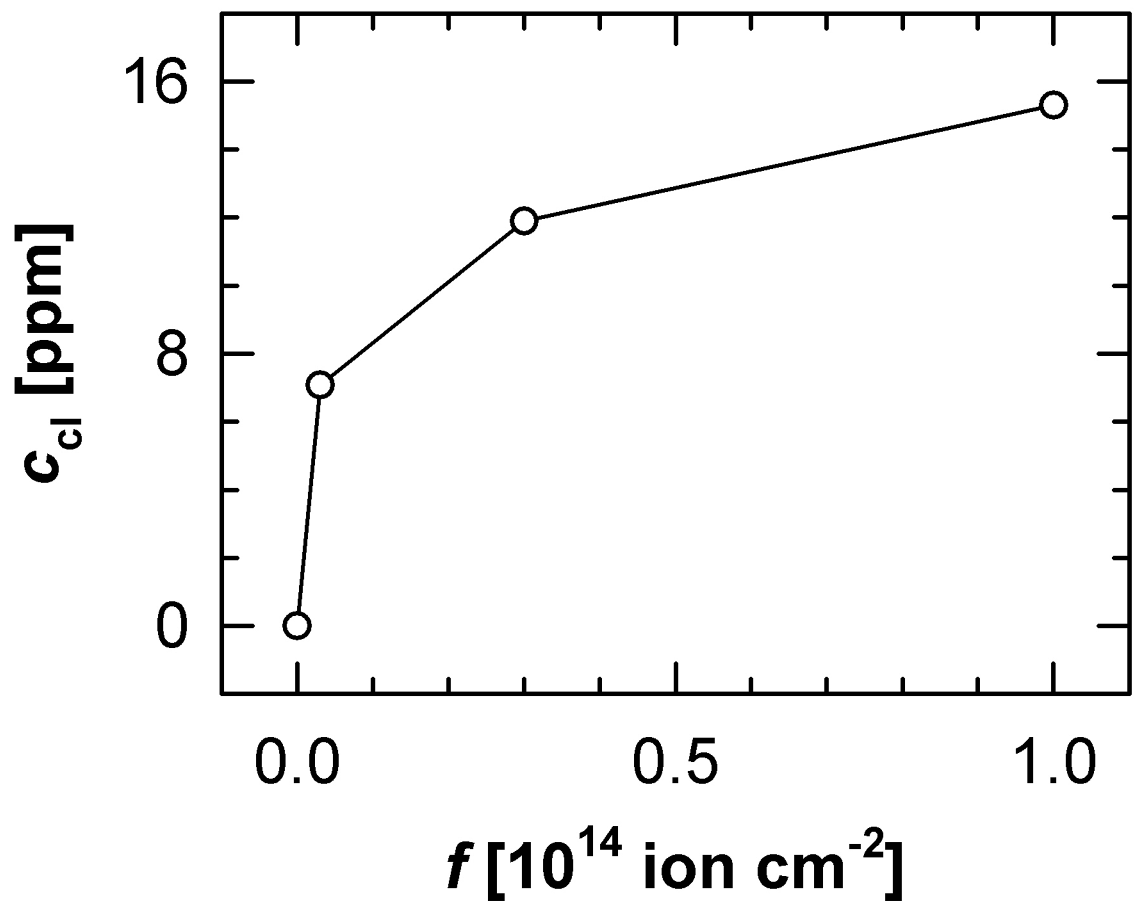

Results & discussion

OT measurements

- Suppressed transmittance for implanted samples in 400 to 550 nm wavelength (2.1 to 3.1 eV) region – probably due to irradiation induced $V_{Zn} – V_O$ (H^+) and clusters (Xe^{26+}),
- trend toward saturation with increasing Xe fluency.

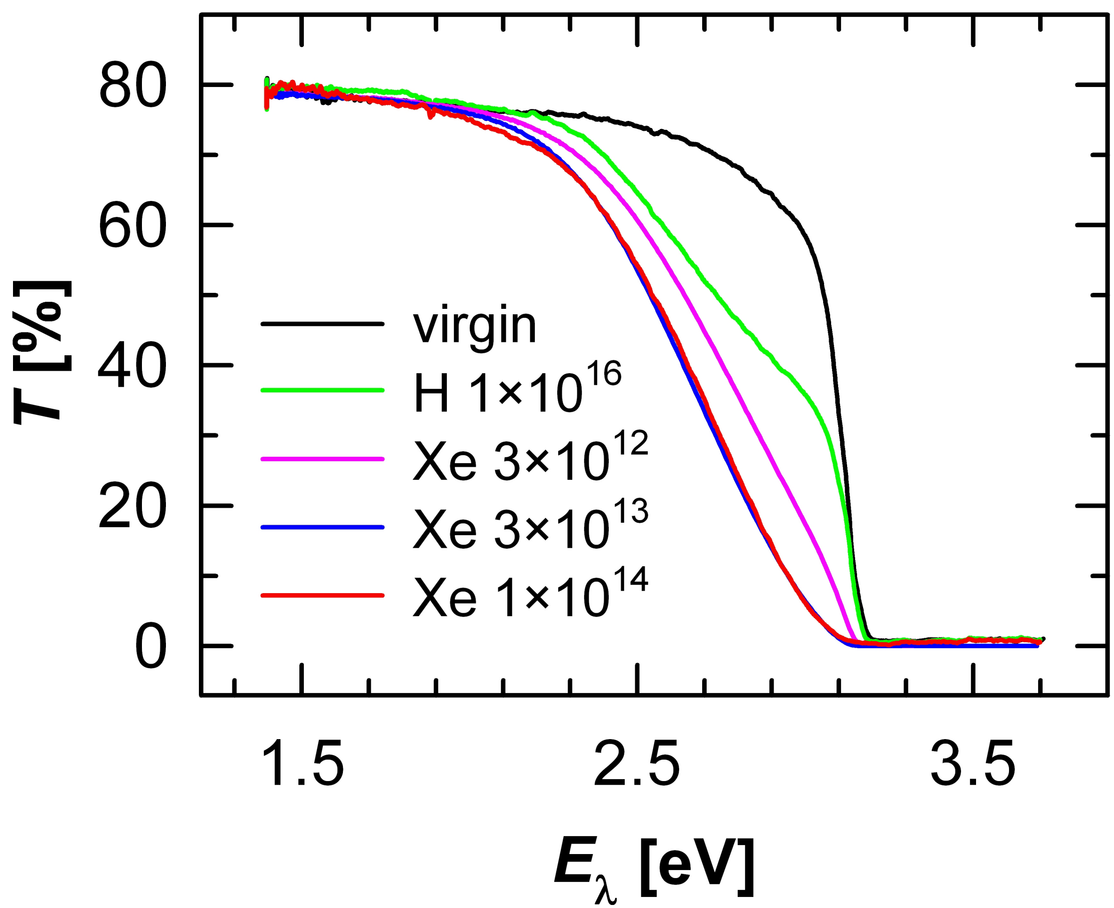

Results & discussion

OT measurements

- Suppressed transmittance for implanted samples in 400 to 550 nm wavelength (2.1 to 3.1 eV) region – probably due to irradiation induced $V_{Zn} – V_O$ (H^+) and clusters (Xe^{26+}),
- red shift of ΔT_{max} for Xe.

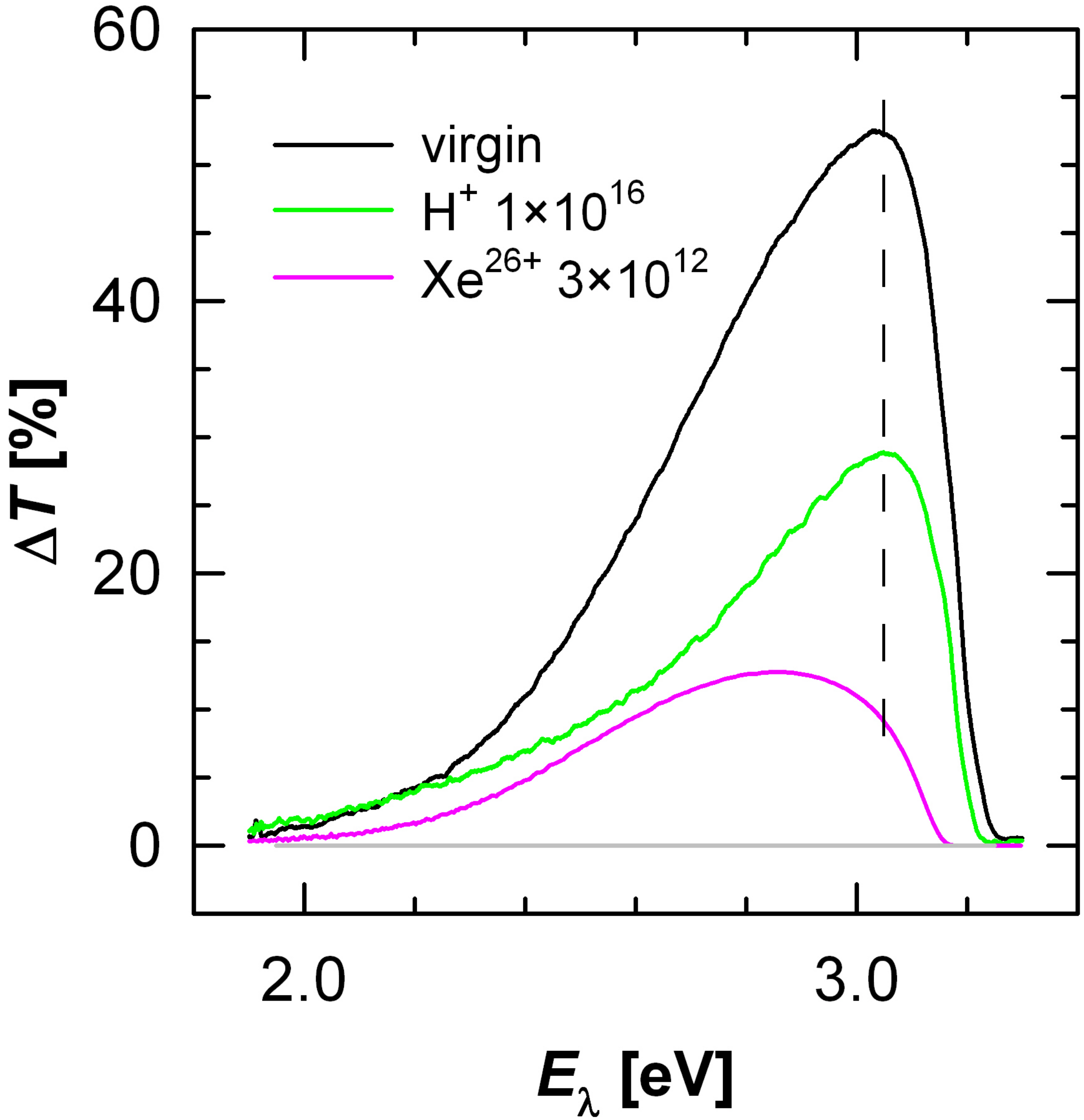

Results & discussion

OT measurements – Tauc plot

squared absorption coefficient α^2
vs
photon energy E_λ

Optical band gap energies E_g^{opt}

- E_g^{opt}-values are lower than the electronic band gap energy (3.37 eV) – optically active defects are present in both samples.
- Xe^+-irradiation – lowering of E_g^{opt} is even larger

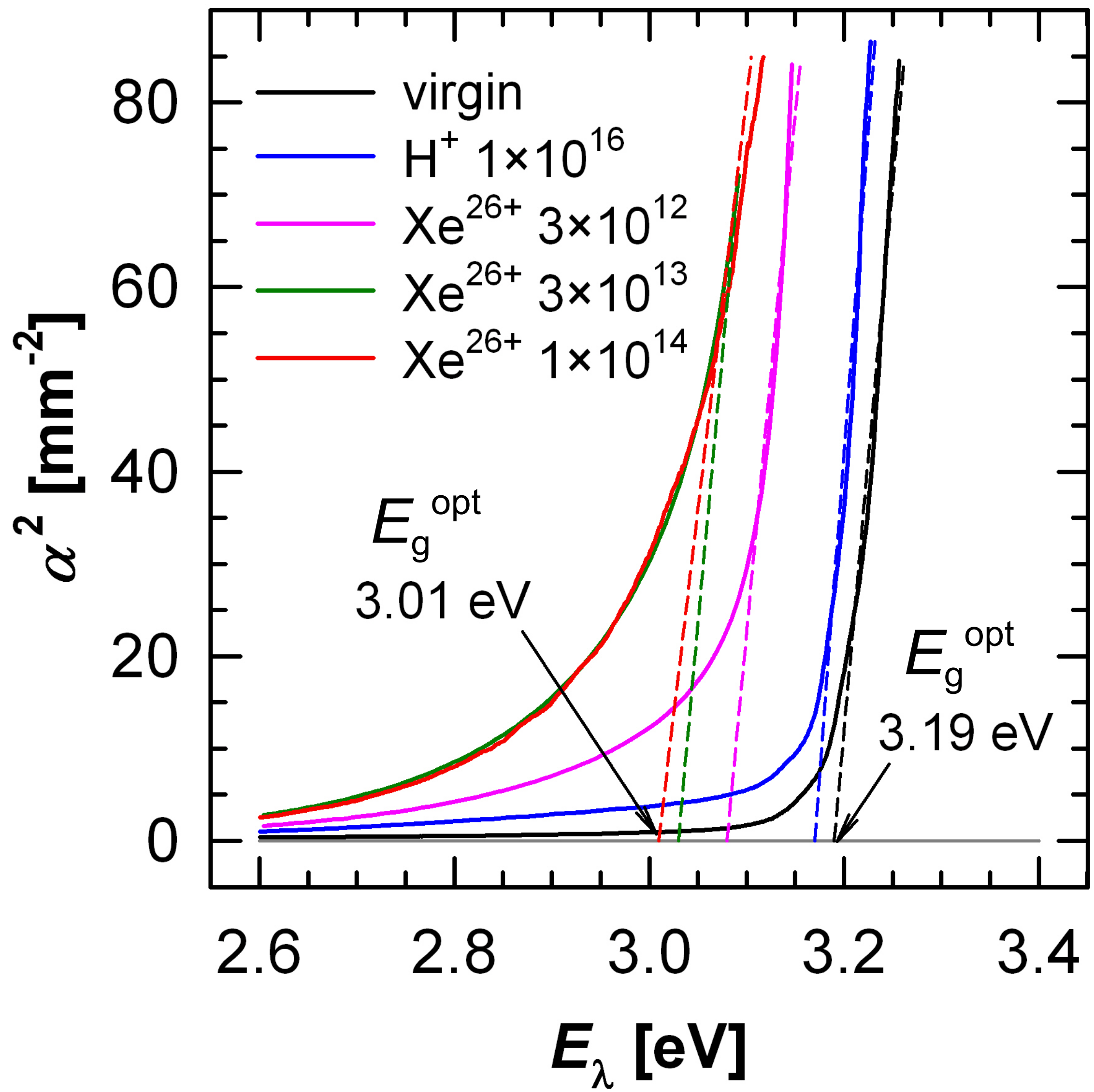

Results & discussion

PL measurements

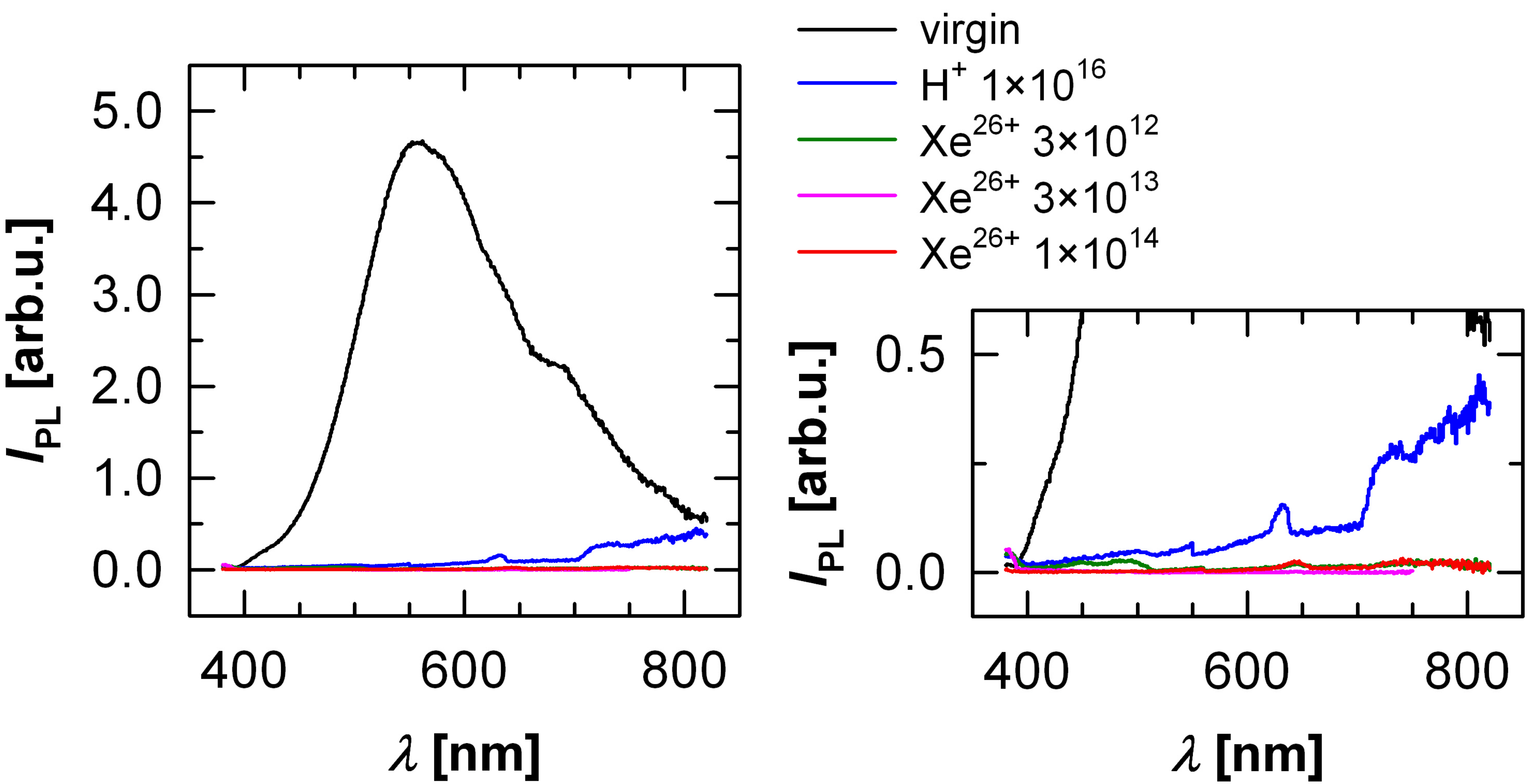

- A well-known green emission (GE) band with a broad maximum at ≈ 550 nm, seen in the virgin sample, is strongly suppressed in the implanted samples.

Results & discussion

PL measurements

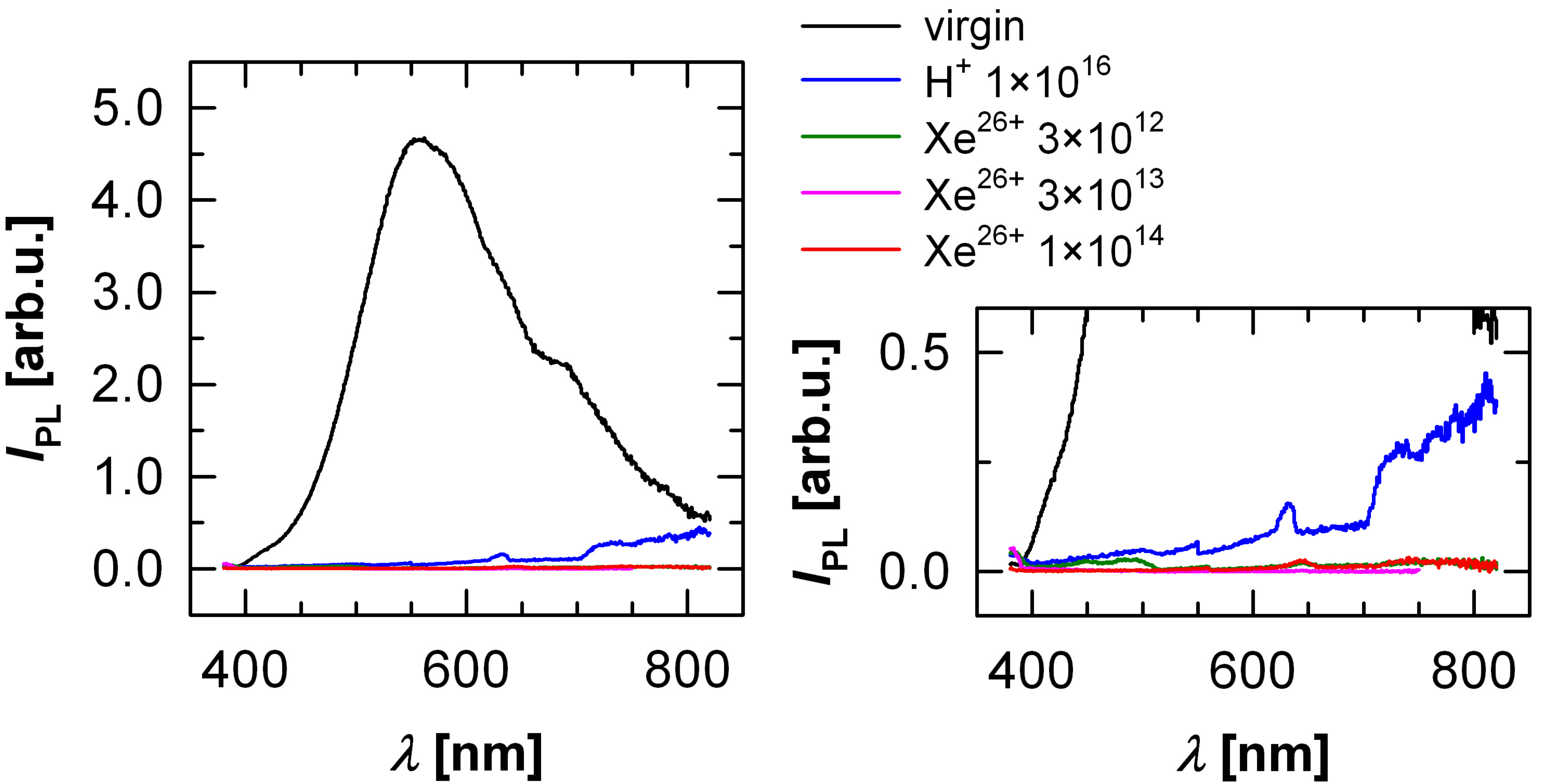

- The GE is quenched by implantations due to irradiation induced defects (V_{Zn}–V_O , vacancy clusters) providing channels for non-radiative recombination of charge carriers.

Summary

- HTG ZnO single crystals were implanted with 2.5 MeV protons to a fluency of 10^{16} cm^{-2} and 167 MeV Xe^{26+} ions to fluencies of 3×10^{12}, 3×10^{13} and 1×10^{14} cm^{-2}.
- The as-grown as well as irradiated crystals were studied by means of positron annihilation techniques (LT, CDB and SPIS) combined with optical methods (OT and PL).
- The grown in V_{Zn} – 1H defects were observed in both the non-irradiated as well as irradiated samples.
- Irradiation induced V_{Zn} – V_O divacancies were identified in proton implanted samples.
- Clusters of ≈10 vacancies were identified in samples irradiated by Xe^{26+} ions and cluster concentrations were estimated.

Summary

- A significant suppression of transmittance in the 400 to 550nm region was found in the H^+- and Xe^{26+}-irradiated ZnO.
- Optical band gaps were deduced from OT measurements. They appear to be lower than the electronic band gaps, indicating thus presence of optically active defects in both implanted samples.
- The GE band is well seen in the virgin sample, but is strongly quenched after proton and Xe implantation, what is likely a result of implantation induced defects which provide a channel for non-radiative recombination of charge carriers.
- A combination of positron annihilation techniques with optical methods can correlate irradiation-induced changes of optical properties with irradiation-created defects.

Acknowledgements

- The Czech Science Foundation for financial support from the project P108/11/0958.
- The PSD-14 organisers for providing possibility to participate in the Conference and present here our results.
- The PSD-14 auditory for patient listening.

Thank you for your attention !

The End